

anharmonic effects²⁰ these ratios should be of the same order as the ratios of their respective characteristic frequencies $\nu_{\Theta} \propto (f/m)^{1/2}$ which, as Table II shows, is indeed the case. Figure 1 illustrates the similarities involved in these ratios.

An explanation of the observed splitting as due to an isotope effect could possibly be justified for germanium on the basis of its stable isotope abundance. This explanation, however, clearly must fail for silicon and diamond because suitable stable isotopes are not present in sufficient abundance for these elements.

We have observed an appreciable shift of all bands to higher frequencies with accompanying decrease in the

extinction coefficient on going to low temperatures, as is common for covalent materials.

It is interesting to note that the extrapolation of the absorption versus temperature curves to $T=0^{\circ}\text{K}$ show positive intercepts, which is in accord with the approach of Lax and Burstein.⁴

ACKNOWLEDGMENTS

We are grateful for helpful discussions with Professor R. C. Locrd, Dr. A. G. Emslie and Dr. S. Shapiro. In addition, we wish to thank D. E. Breen who was involved in some of the early measurements. We are further indebted to Dr. J. N. Plendl of the U. S. Air Force Cambridge Research Laboratories for initiating and stimulating this research and to L. C. Mansur for his assistance.

²⁰ J. N. Plendl, Phys. Rev. **123**, 1172 (1961).

Saturation Magnetoresistance and Impurity Scattering Anisotropy in *n*-Type Silicon*

L. J. NEURINGER

National Magnet Laboratory, Massachusetts Institute of Technology, Cambridge, Massachusetts†

AND

DONALD LONG

Honeywell Research Center, Hopkins, Minnesota

(Received 9 March 1964)

In the classical strong-field region the magnetoresistance of semiconductors is expected to saturate. If one investigates the dependence of the saturation magnetoresistance upon impurity concentration, i.e., upon the strength of ionized-impurity scattering, quantitative conclusions may be drawn concerning the anisotropy of the relaxation time for such scattering. The strong-field longitudinal magnetoresistance and carrier mobility of phosphorus-doped silicon have been studied in dc magnetic fields to 90 kG at 78°K. Measurements were made on a series of [111]-oriented samples covering the doping range 2×10^{13} – 6×10^{16} phosphorus atoms/cm³. A quantitative analysis has been made involving Maxwellian averages over carrier energy and relaxation times that combine the impurity, intravalley, and intervalley scattering mechanisms. The strength of the impurity scattering in each sample was taken to be μ_L/μ where μ_L is the known lattice scattering mobility and μ is the conductivity mobility determined from the measured value of R_{∞}/ρ , the ratio of the strong field Hall coefficient to the resistivity. The data agree very well with the theory of Samoilovich, Korenblit, and Dakhovskii (SKD). In the more heavily doped samples, above 10^{16} phosphorus atoms/cm³, the effects of neutral impurity scattering are observed.

I. INTRODUCTION

THE electrical properties of a semiconductor are governed by the electronic energy band structure and by the various processes which scatter the electrons. In the semiconductors which have been most extensively studied, such as silicon and germanium, a detailed picture of the energy bands has been obtained and the major scattering mechanisms have been defined. However, our knowledge regarding the scattering strengths

and anisotropies is more limited. This is partially due to the fact that galvanomagnetic effects such as magnetoresistance, while sensitive to the type of scattering, involve complicated averages over relaxation times of the carrier when measured in normal laboratory magnetic fields. The magnetoresistance has therefore been used primarily to identify the directions of energy extrema in *k* space and to find ratios of the components of the effective mass tensor. The situation is very much altered in the classical strong-field limit.

One of the distinctive features of the galvanomagnetic properties of semiconductors in the classical strong-field region is saturation of the magnetoresistance and Hall

* Most of this work was done at the Raytheon Research Division, Waltham, Massachusetts.

† Supported by the U. S. Air Force Office of Scientific Research.

coefficient. This effect has been observed at strong magnetic fields exceeding 50 kG in germanium¹⁻³ and in silicon.⁴ However, the results were interpreted in a qualitative fashion in terms of the conduction band-energy spheroid anisotropy parameter. Such an approach is rigorously correct only if a single type of scattering mechanism is important. In general it is necessary to use the more complete expressions of Herring and Vogt⁵ involving Maxwellian averages over the carrier energy and relaxation times which combine the impurity, intravalley, and intervalley scattering mechanisms. In this way, the strong-field data can be analyzed in a manner such as to yield definite information concerning the scattering strengths and anisotropies.

Earlier experimental studies of scattering effects in *n*-type silicon⁶ involved Hall and magnetoresistance measurements in relatively weak magnetic fields below 25 kG. As a consequence, these investigations were restricted to relatively pure samples and were somewhat hampered by lack of true saturation. While quantitative conclusions were derived by Long and Myers⁶ concerning the lattice scattering strengths and anisotropies, very little could be said about the impurity scattering component both with regard to its magnitude and variation with impurity content. The purpose of this paper is to present the results of a quantitative analysis of the dependence upon the strength of the impurity scattering of the strong-field longitudinal magnetoresistance in *n*-type silicon at 78°K.

The advantages of investigating galvanomagnetic phenomena in *n*-type silicon at classical saturation stem from two considerations. First, the Herring and Vogt formulas become simplified in the limit of infinite fields. Second, by using the saturation value of the Hall coefficient one ascertains the actual conductivity mobility, free of the uncertainties encountered at weak fields which arise from the variation of the Hall coefficient factor with field. Thus, in the present work, an *experimentally* determined measure of the strength of impurity scattering is used in the form μ_L/μ , where μ_L is the lattice scattering mobility⁷ and μ is the conductivity mobility determined from the ratio of the Hall coefficient at infinite field to the resistivity, R_∞/ρ . Our main objective is to compare with theoretical predictions^{5,8,9} the experimental dependence of $\rho(H)/\rho(O)]_{111, H \rightarrow \infty}$

upon μ_L/μ as the impurity concentration is varied. The available theories^{8,9} use the Born approximation to calculate the ionized-impurity scattering relaxation times, τ_\perp and $\tau_{||}$, for conduction perpendicular and parallel to a constant-energy spheroid axes in terms of the spheroid mass anisotropy.

It should be recognized that in this work only the longitudinal magnetoresistance is considered, because it is generally far less sensitive than the transverse magnetoresistance to surface damage, sample inhomogeneities, and other extraneous influences.^{10,11}

II. EXPERIMENTAL RESULTS

The experimental work was performed at the MIT National Magnet Laboratory using a 2-in. air core Bitter solenoid which generates 90 kG at a magnetizing current of 10 kA.

All the samples were taken from float-zone crystals. After orientation and cutting, the samples were ground, lapped, and then etched in CP4 solution. Gold wires of 3-mil diam were alloyed into the specimen in a manner to ensure minimum contact area at the resistivity and Hall probes in order to avoid electrode effects.

Various experimental techniques were employed to check the reproducibility and reliability of the data. We have taken the precaution of studying only samples having a large length to transverse dimension ratio in order to minimize size effects.⁴ Some of the purer samples were checked for homogeneity by measuring the magnetoresistance and Hall coefficient at different positions along the sample. Furthermore, the important question as to the influence of the type of surface treatment was answered by performing several experiments with sandblasted specimens. No difference in the values of the saturation magnetoresistance were found between etched and sandblasted surfaces.

The effective mass parameters of silicon and the orientation of the sample with respect to the energy ellipsoids of the conduction band are shown in Fig. 1.

The experimental saturation data at 78°K of the eight samples studied are exhibited in Fig. 2. The range of phosphorus impurity concentration varies from approximately 2×10^{13} atoms per cm³ for sample SP6S to 6×10^{16} atoms per cm³ for sample D8-3. A summary of the electrical characteristics of the samples is presented in Table I. An important feature of this work is the measurement above 50 kG of the saturation Hall coefficient, R_∞ , of the samples in Fig. 2. This allows a direct experimental evaluation of the conductivity mobility as determined by the mixed lattice and impurity scattering. These parameters are also entered in Table I. The donor and acceptor impurity concentrations, N_D and N_A , in each sample are given in the last two columns of Table I. These values were determined

¹ H. P. Furth and R. W. Wanick, Phys. Rev. **104**, 343 (1956).

² W. F. Love and W. F. Wei, Phys. Rev. **123**, 67 (1961).

³ L. J. Neuringer, H. Roth, and W. D. Straub, Bull. Am. Phys. Soc. **7**, 330 (1962).

⁴ L. J. Neuringer and W. J. Little, *Proceedings of the International Conference on the Physics of Semiconductors, Exeter, 1962* (The Institute of Physics and the Physical Society, London, 1962), p. 614.

⁵ C. Herring and E. Vogt, Phys. Rev. **101**, 944 (1956).

⁶ D. Long and J. Myers, Phys. Rev. **120**, 39 (1960).

⁷ D. Long, Phys. Rev. **120**, 2024 (1960).

⁸ A. G. Samoilovich, I. Ya. Korenblit, and I. V. Dakhovskii, Dokl. Akad. Nauk SSSR **139**, 355 (1961) [English transl.: Soviet Phys.—Doklady **6**, 606 (1962)]; referred to as SKD in the text.

⁹ F. S. Ham, Phys. Rev. **100**, 1251 (1955).

¹⁰ C. Herring, T. H. Geballe, and J. E. Kunzler, Bell System Tech. J. **38**, 657 (1959).

¹¹ C. Herring, J. Appl. Phys. **31**, 1939 (1960).

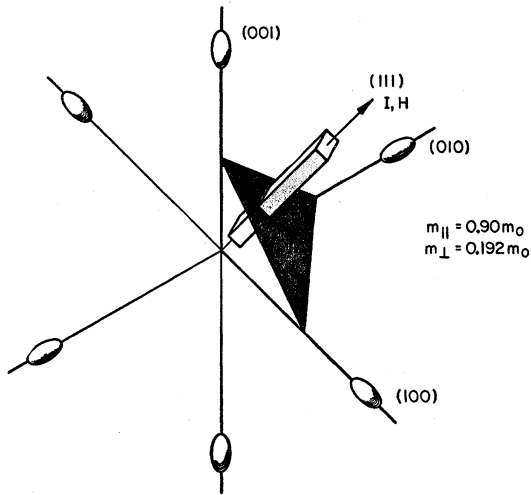


FIG. 1. Orientation of the samples with respect to the conduction-band ellipsoids. The ellipsoid mass parameter values for n -type silicon are indicated.

from a conventional analysis of the dependence of the Hall coefficient on temperature in the impurity ionization range. The conductivity mobility is plotted as a function of the ionized-impurity concentration N_I at 78°K in Fig. 4.

III. ANALYSIS

The analysis which follows will proceed in two parts. First, the saturation magnetoresistance will be analyzed in terms of the over-all relaxation time anisotropy, to which it is highly sensitive. From this analysis information about the ionized-impurity scattering anisotropy will be obtained. Then we shall use the measured

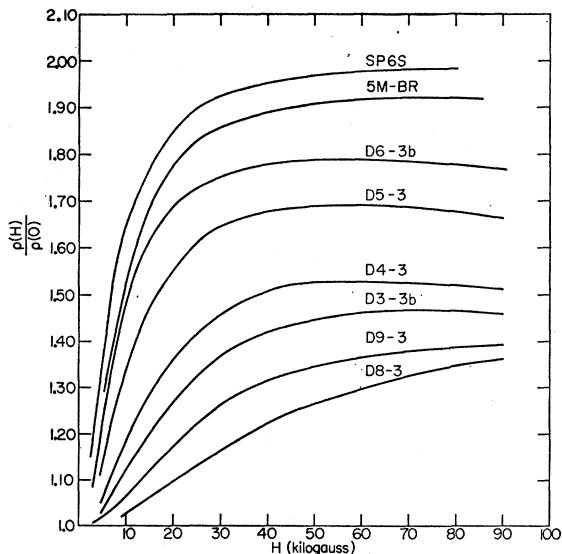


FIG. 2. Longitudinal magnetoresistance at 78°K as a function of magnetic field H along the [111] direction for several impurity concentrations.

conductivity mobility to check the consistency of the magnetoresistance analysis, particularly with respect to the magnitude of the impurity scattering.

A. Magnetoresistance

Our purpose here is to confront the theory with the dependence of $\rho(H)/\rho(O)$ at saturation upon the strength of impurity scattering. As an index of the amount of impurity scattering we use the experimentally measured value of μ_L/μ , the ratio of lattice scattering mobility⁷ to the conductivity mobility, governed by mixed lattice and impurity scattering. This comparison is noteworthy in that no adjustable parameters are involved. The lattice scattering strengths and anisotropies are those deduced previously by Long,^{6,7} and the impurity scattering anisotropy is taken from the theories of SKD⁸ and of Ham.⁹

The Herring and Vogt formalism describes transport effects in a many-valley semiconductor like n -type silicon and takes scattering anisotropy into account. The scattering is described by a diagonal relaxation-time tensor with components, τ_{ii} , one for each principal direction of a constant-energy ellipsoid. Anisotropy in the scattering is represented by differences in the values of the τ_{ii} . For n -type silicon they reduce to two independent components τ_{\perp} and τ_{\parallel} , since the constant-energy surfaces are ellipsoids of revolution or spheroids. The subscript \parallel (\perp) indicates the direction parallel (perpendicular) to the spheroid axis. The Herring-Vogt approach is justified if all the scattering mechanisms either conserve carrier energy or randomize carrier velocities, and this is the case for the lattice and impurity scattering mechanisms in the samples studied. Furthermore, this theory gives very accurate results if the over-all τ anisotropy for any mixtures of scattering mechanisms under consideration is not too extreme; thus, the over-all τ should not vary over the constant-energy surface by more than about a factor of 2. This condition was easily satisfied in all the experimental cases considered here.

According to the Herring-Vogt model the saturation value of the longitudinal magnetoresistance of n -type silicon in a [111] direction is given by

$$\left. \frac{\rho(H)}{\rho(O)} \right]_{111, H \rightarrow \infty} = \frac{\left[\frac{2\langle \epsilon \tau_{\perp} \rangle}{m_{\perp}} + \frac{\langle \epsilon \tau_{\parallel} \rangle}{m_{\parallel}} \right]}{9 \left\langle \frac{\epsilon}{(2m_{\perp}/\tau_{\perp}) + (m_{\parallel}/\tau_{\parallel})} \right\rangle}, \quad (1)$$

where $(\rho(H)/\rho(O))_{111, H \rightarrow \infty}$ is the ratio of the sample resistivities in infinite and zero magnetic fields, and the $\langle \rangle$ brackets represent Maxwellian averages over the carrier energy ϵ . Equation (1) assumes absence of energy-level quantization effects. The condition is presumably satisfied in our experiments inasmuch as the quantity $\frac{1}{2}\hbar\omega/kT$ is equal to 0.28 for all conduction

TABLE I. Summary of sample properties.

Sample ^a	300°K		78°K				Impurity concentrations	
	Resistivity (Ohm-cm)	Weak-field ^b Hall coefficient R_0 , (cm ³ /C)	Resistivity (Ohm-cm)	Weak-field ^c Hall coefficient R_0 , (cm ³ /C)	Strong-field Hall coefficient R_{∞} , (cm ³ /C)	Conductivity mobility $\mu = R_{\infty}/\rho$ (cm ² /V-sec)	N_D (cm ⁻³)	N_A (cm ⁻³)
D8-3	0.134	1.15×10^3	0.167	5.51×10^3	5.76×10^3	3.45×10^3	$\sim 6.5 \times 10^{16}$	$< 10^{14}$
D9-3	0.215	2.27×10^3	0.160	7.85×10^3	8.34×10^3	5.21×10^3	3.3×10^{16}	$< 10^{14}$
D3-3b	0.476	5.88×10^3	0.196	1.55×10^3	1.69×10^3	8.62×10^3	1.3×10^{16}	8.7×10^{12}
D4-3	1.06	1.36×10^3	0.269	2.59×10^3	2.85×10^3	1.06×10^4	6.1×10^{15}	1.7×10^{13}
D5-3	5.14	7.33×10^3	0.666	8.50×10^3	1.00×10^4	1.50×10^4	1.2×10^{15}	1.1×10^{14}
D6-3b	14.9	2.17×10^4	1.37	2.14×10^4	2.55×10^4	1.86×10^4	3.9×10^{14}	3.7×10^{13}
5M-BR	57.9	9.65×10^4	4.66	8.51×10^4	9.52×10^4	2.05×10^4	1.3×10^{14}	1.7×10^{13}
SP6S	21.8	4.61×10^5	4.91×10^5	2.25×10^4	2.1×10^{13}	0.8×10^{13}

^a Bar-shaped samples, except for 5M-BR which was Type A bridge-shaped as in Ref. 4.

^b Measured at 1.0 kG for all samples, except D8-3 and D9-3 which were measured at 2.52 kG. The Hall coefficient of samples D3-3b to SP6S was also measured at 0.5 kG and agreed with the 1.0 kG data to within 2%.

^c Measured at 0.5 and 1.0 kG for all samples; both sets of data agreed to within 3%.

band ellipsoids at 90 kG and 78°K, and inasmuch as good saturation is observed.

The carrier mobility μ is given by

$$\mu = \frac{q}{3\langle \epsilon \rangle} \left[\frac{2\langle \epsilon \tau_{\perp} \rangle}{m_{\perp}} + \frac{\langle \epsilon \tau_{\parallel} \rangle}{m_{\parallel}} \right], \quad (2)$$

where q is the electronic charge.

In deriving the τ_{\parallel} and τ_{\perp} values needed for computing the Maxwellian averages appearing in Eqs. (1) and (2) we follow the prescription⁵

$$\frac{1}{\tau_{\perp}} = \frac{1}{\tau_{\perp A}} + \frac{1}{\tau_{\perp IV}} + \frac{1}{\tau_{\perp I}}, \quad (3a)$$

$$\frac{1}{\tau_{\parallel}} = \frac{1}{\tau_{\parallel A}} + \frac{1}{\tau_{\parallel IV}} + \frac{1}{\tau_{\parallel I}}, \quad (3b)$$

where subscripts A, IV, and I refer to acoustic mode intravalley lattice scattering, intervalley lattice scattering, and ionized-impurity scattering, respectively. The number of independent variables implicit in the Eqs. (3a) and (3b) is reduced by use of the information available as to the scattering anisotropies and relative strengths of the three mechanisms of importance at 78°K. The lattice scattering relaxation times of Eq. (3b) are fixed relative to Eq. (3a) by the conditions^{6,7}

$$\frac{\tau_{\parallel}}{\tau_{\perp}} \Big|_A = \frac{2}{3}, \quad \frac{\tau_{\parallel}}{\tau_{\perp}} \Big|_{IV} = 1. \quad (4)$$

The Maxwellian averages will be calculated for two values of the impurity scattering anisotropy, $(\tau_{\parallel}/\tau_{\perp})_I = 3$ and $(\tau_{\parallel}/\tau_{\perp})_I = 4$, which tend to bracket the predictions of the theories of SKD and Ham. Even with the use of Eq. (4) there still appear three coupling constants in the lattice scattering portion of Eq. (3a), arising from intravalley acoustic scattering and from intervalley scattering by two phonons of characteristic temperatures 190 and 630°K. These three coupling

constants are further reduced to a single one because one knows the ratios of the coupling constants of the characteristic phonons responsible for intervalley lattice scattering to the coupling constant for acoustic scattering for conduction perpendicular to an energy spheroid axis. In terms of this single coupling constant, the acoustic and intervalley lattice scattering contributions are written as

$$\frac{1}{\tau_{\perp A}} = w_{A1} \left(\frac{\epsilon}{kT_0} \right)^{1/2} \left(\frac{T}{T_0} \right), \quad (5)$$

$$\begin{aligned} \frac{1}{\tau_{\perp IV}} &= 2w_{A1} \left(\frac{630}{T_0} \right)^{3/2} \\ &\times \left[\frac{((\epsilon/630k) + 1)^{1/2}}{\exp(630/T) - 1} + \frac{((\epsilon/630k) - 1)^{1/2} \text{ or } 0}{1 - \exp(-630/T)} \right] \\ &+ 0.15w_{A1} \left(\frac{190}{T_0} \right)^{3/2} \\ &\times \left[\frac{((\epsilon/190k) + 1)^{1/2}}{\exp(190/T) - 1} + \frac{((\epsilon/190k) - 1)^{1/2} \text{ or } 0}{1 - \exp(-630/T)} \right], \quad (6) \end{aligned}$$

where w_{A1} is the coupling constant for acoustic scattering, and T_0 is a reference temperature. In the foregoing manner Eqs. (3a) and (3b) have been reduced so as to possess only two independent parameters, the coupling constant for acoustic scattering w_{A1} and a coupling constant for ionized-impurity scattering. These expressions are known to give a good description of the galvanomagnetic effects in n -type silicon.⁷

The two solid curves plotted in Fig. 3 were constructed by calculating the three Maxwellian averages for a number of strengths of impurity scattering relative to the lattice scattering. The necessary integrals were evaluated numerically using Simpson's rule. For the $\tau_{\perp I}$ and $\tau_{\parallel I}$ contributions, it was assumed that the ionized-impurity scattering relaxation times depend on carrier

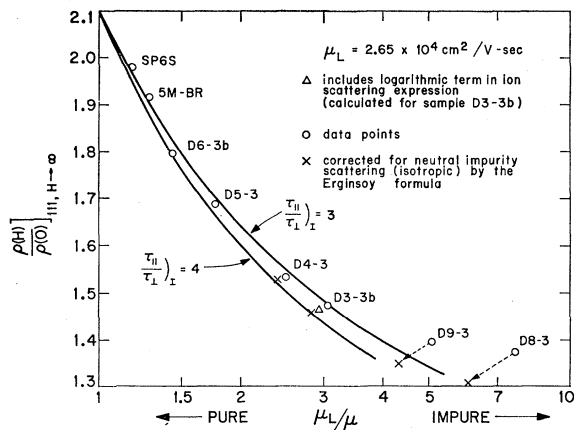


FIG. 3. Saturation longitudinal magnetoresistance for the [111] direction versus strength of impurity scattering, as represented by μ_L/μ . The solid curves were calculated using the procedure described in Sec. III.1. The value of lattice scattering mobility at 78°K used throughout is indicated.

energy as $\tau_l \propto \epsilon^{3/2}$, thereby neglecting the weak dependence on carrier energy of the logarithmic term appearing in the usual expressions for τ_l .^{12,13} The upper solid curve is constructed under the assumption that $(\tau_{11}/\tau_l)_I = 3$, and the lower curve is for $(\tau_{11}/\tau_l)_I = 4$. The abscissa values in Fig. 3 were determined by taking the ratios of the mobility of Eq. (2) for pure lattice scattering μ_L to the mobilities μ determined from the same equation for the various strengths of impurity scattering. Note that it was never necessary to be concerned about normalizing the Maxwellian averages to any particular value, because they always appear in ratios in the expressions for the ordinate and abscissa of Fig. 3.

According to the analysis of SKD the value of $(\tau_{11}/\tau_l)_I$ for *n*-type silicon should decrease very slowly as a function of increasing impurity concentration from a maximum value of 3.56 in the limit of pure material. The two solid curves in Fig. 3 tend to bracket the expected theoretical behavior. The open triangle in Fig. 3 represents the result of an additional calculation for sample D3-3b in which was included the logarithmic function of carrier energy in the expressions for τ_l and τ_{11} and the particular value of $(\tau_{11}/\tau_l)_I$ predicted by SKD's results. It is seen that the triangle lies between the two solid curves, so that there is very little error involved in neglecting the logarithmic terms. It is important to realize that the slow decrease of the $(\tau_{11}/\tau_l)_I$ ratio with increasing impurity concentration predicted by SKD is directly related to the logarithmic term. This term represents the effects of the shielding of the impurity charge center by the carriers. And the decrease of the effective shielding radius with increasing

carrier density tends to diminish the scattering anisotropy.

The calculated results presented as the solid curves and the triangle in Fig. 3 are entirely independent of the experimental data. The data points, which represent the saturation magnetoresistance values of Fig. 2 and the conductivity mobilities listed in Table I, are in good agreement with the calculated results. The points for samples D9-3 and D8-3, however, exhibit an appreciable deviation. It is believed that in these samples, which are uncompensated, the deviation arises from a large contribution of *neutral* impurity scattering. Accordingly, the data points for the most pure samples have been corrected by subtracting the neutral impurity scattering contribution as follows. Neutral impurity scattering is isotropic, and its relaxation time τ_N is independent of energy and temperature. The Erginsoy formula¹⁴

$$1/\tau_N = (20\hbar^3\kappa/m_1^*q^2m_2^*)N_n \quad (7)$$

was used to calculate τ_N for each sample. In Eq. (7) κ is the dielectric constant, m_1^* is an effective mass deduced from the known ground-state energy of the hydrogen-like donor impurities (~ 0.044 eV), $m_2^* = (m_1m_2^2)^{1/3}$, and $N_n = \{(N_D - N_A) - n\}$ is the density of neutral impurities. The necessary correction was determined by using Eqs. (1) and (2) to calculate $(\rho(H)/\rho(O))_{[111], H \rightarrow \infty}$ and μ with and without the neutral impurity scattering contribution. This was done by adding $1/\tau_N$ to $\langle \epsilon \rangle / \langle \epsilon \tau_{11} \rangle$ and to $\langle \epsilon \rangle / \langle \epsilon \tau_l \rangle$, which is a good approximation because τ_N is independent of energy. The differences in the resulting values indicated the necessary corrections to the ordinate and abscissa for samples D4-3, D3-3b, D9-3 and D8-3. The adjusted values are indicated by the crosses in Fig. 3 and agree with the theoretical curves.

A similar analysis was applied to the saturation magnetoresistance data for [110]-oriented samples reported by Neuringer and Little,⁴ using the appropriate analog⁵ of Eq. (1). In these samples the variation of the saturation longitudinal magnetoresistance with impurity concentration is much smaller than for the [111]-oriented samples and therefore is not as sensitive a test of the theory. Nevertheless, the model discussed in this section gave a satisfactory description of the [110] data, thereby demonstrating the general validity and consistency of the analysis.

B. Conductivity Mobility

In this section the conductivity mobility is treated by means of an approximate formula which takes the mass anisotropy into account correctly but which averages out the relaxation-time anisotropy. This type of treatment is felt to be satisfactory, because (1) the mobility itself is an inherently isotropic quantity, (2) it is much less sensitive to mass and scattering anisotropies than the magnetoresistance, and (3) the anisot-

¹² D. Long, Phys. Rev. **129**, 2464 (1963).

¹³ F. J. Blatt, *Solid State Physics*, edited by F. Seitz and D. Turnbull (Academic Press Inc., New York, 1957), Vol. 4, pp. 199-366.

¹⁴ C. Erginsoy, Phys. Rev. **79**, 1013 (1950).

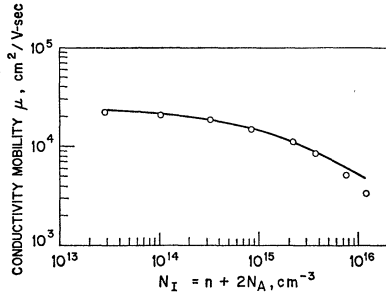


FIG. 4. Conductivity mobility $\mu = R_{\infty}/\rho$ as a function of the concentration of ionized impurities at 78°K in the n -type silicon samples. The points represent data, and the solid curve is the result of a calculation described in Sec. III. B.

ropy of the over-all relaxation time in our experiments was always much less than of the effective mass. Thus, the isotropic approximation should be valid and obviates the very laborious procedure of taking the scattering anisotropy into account to calculate the mobility. It should be noted that the small amount of intervalley lattice scattering present in the samples at 78°K is neglected in the mobility analysis. All the lattice scattering is simply assumed to have the character of ordinary acoustic intravalley scattering. This approximation is also adequate for the mobility analysis.

The dependence of the observed conductivity mobility upon the concentration of ionized impurities is displayed in Fig. 4 by the open circles. The solid curve represents the calculated mobility for the samples according to their ionized-impurity concentrations at 78°K. For concentrations less than 10^{16} cm^{-3} the SKD formula for the ionized-impurity scattering mobility can be written as¹²

$$\mu_I \cong \frac{7.5 \times 10^{17} T^{3/2}}{N_I (\ln b - 1.20)} \text{ cm}^2/\text{V-sec}, \quad (8)$$

where N_I is the concentration of ionized impurities and b is a shielding factor.

The solid curve of Fig. 4 represents a calculation of the conductivity mobility as a function of N_I . In

obtaining this curve μ_I was calculated by means of Eq. (8), and then a mobility μ' due to combined lattice and ionized-impurity scattering was obtained by using the relationship¹⁵

$$\mu' = \mu_L (1 + \chi^2 \{ C_i \chi \cos \chi + S_i \chi \sin \chi - \frac{1}{2} \pi \sin \chi \}), \quad (9)$$

where $\chi^2 = 6(\mu_L/\mu_I)$. Finally, neutral impurity scattering μ_N was calculated from Eq. (7) and the mobility used in comparison with data is $\mu^{-1} = (\mu')^{-1} + (\mu_N)^{-1}$. It can be seen in Fig. 4 that the calculated curve agrees very well with the data points where agreement can be expected, namely at concentrations less than 10^{16} cm^{-3} .

IV. CONCLUSIONS

It has been shown that accurate and reliable magnetoresistance data in the classical saturation regime may be obtained using strong dc magnetic fields and suitable precautions in sample preparation. Excellent agreement is attained between experiment and theoretical predictions as is evident in Figs. 3 and 4 for all the samples except the two most heavily doped ones. This indicates that the classical strong-field theory of Herring and Vogt and the use of the Born approximation lead to an entirely adequate description of the ionized-impurity scattering and its anisotropy in n -type silicon at 78°K for concentrations as high as 10^{16} cm^{-3} . Furthermore, the agreement in the case of the two least pure samples is satisfactory, indicating that the theory is still reasonably good up to 6×10^{16} cm^{-3} . No conclusive evidence of the very slight decrease of $(\tau_{II}/\tau_I)_I$ with increasing impurity concentration predicted by the theory can be extracted from Fig. 3 because that trend is masked by even the very small scatter in the data.

ACKNOWLEDGMENTS

We wish to thank the National Magnet Laboratory, MIT for the use of their facility, and Dr. W. C. Dunlap and Dr. O. N. Tufte for a critical reading of the manuscript. We are also grateful to Dr. H. Roth for the use of his apparatus to measure the resistivity and weak-field Hall coefficient.

¹⁵ P. P. Debye and E. M. Conwell, Phys. Rev. **93**, 693 (1954).